Electrically induced structure transition in nematic liquid crystal droplets with conical boundary conditions

V. Yu. Rudyak,[1,*] M. N. Krakhalev,[2,3] V. S. Sutormin,[2] O. O. Prishchepa,[2,3] V. Ya. Zyryanov,[2] J.-H. Liu,[4] A. V. Emelyanenko,[1] and A. R. Khokhlov[1]

[1]*Lomonosov Moscow State University, Faculty of Physics, Moscow 119991, Russia*

[2]*Kirensky Institute of Physics, Federal Research Center - Krasnoyarsk Scientific Center, Siberian Branch, Russian Academy of Sciences, Krasnoyarsk 660036, Russia*

[3]*Institute of Engineering Physics and Radio Electronics, Siberian Federal University, Krasnoyarsk 660041, Russia*

[4]*Department of Chemical Engineering, National Cheng Kung University, Tainan, Taiwan*

(Received 6 July 2017; published 6 November 2017)

Polymer-dispersed liquid crystal composites have been a focus of study for a long time for their unique electro-optical properties and manufacturing by "bottom-up" techniques at large scales. In this paper, nematic liquid crystal oblate droplets with conical boundary conditions (CBCs) under the action of electric field were studied by computer simulations and polarized optical microscopy. Droplets with CBCs were shown to prefer an axial-bipolar structure, which combines a pair of boojums and circular disclinations on a surface. In contrast to droplets with degenerate planar boundary conditions (PBCs), hybridization of the two structure types in droplets with CBCs leads to a two-minima energy profile, resulting in an abrupt structure transition and bistable behavior of the system. The nature of the low-energy barrier in droplets with CBCs makes it highly sensitive to external stimuli, such as electric or magnetic fields, temperature, and light. In particular, the value of the electric field of the structure reorientation in droplets with CBCs was found to be a few times smaller than the one for droplets with PBCs, and the droplet state remained stable after switching off the voltage.

DOI: 10.1103/PhysRevE.96.052701

Various orientation structures of the director field can be formed inside liquid crystal (LC) droplets depending on the material parameters, surface anchoring, droplet shape and size, etc. [1–7]. In turn, the optical properties of polymer-dispersed liquid crystal (PDLC) films containing such droplets are determined by the orientational structure. Liquid crystal molecules are oriented by an electric (or magnetic) field that results in the transformation of the orientational structure inside the droplets, and hence, in particular, a change in the optical properties of the whole PDLC film [8–11]. Manipulation by PDLC optical characteristics is used in displays [12,13], light modulators [14], and electrically operated photonic crystals [15–17].

Peculiarities of the structure reorientation within the droplets assign the response parameters (threshold voltage, switching-on and switching-off times, contrast ratio, etc.) of the PDLC film. The aim of the present investigation is to find out the conditions at which the nematic liquid crystal (NLC) droplet structure exhibits an abrupt transition at some applied low critical voltage, while below and above this critical voltage the structure remains almost unchanged.

One of the "easy" configurations, a bipolar one with two point defects, boojums, is formed at the planar boundary condition (PBC) [Fig. 1(a)]. In such droplets, the bipolar axis connecting the boojums is perpendicular to the short ellipsoid axis and parallel to the PDLC film plane [9,18,19]. When the electric field is applied along or perpendicularly to the bipolar axis, several different scenarios of the NLC droplet structure transformation can emerge. In some cases a continuous change in the orientation structure is observed with an increase of voltage exceeding some threshold value [9,19–21]. In other systems the threshold process of structure reorientation begins in the droplet center and propagates gradually into the whole bulk with increasing voltage [22–24], while the location of the boojums remains invariable. In Ref. [25], the operating electric field initially forms a twist wall coinciding with a bipolar axis and disappearing with increasing voltage, so that the bipolar axis becomes oriented along the field. In each case, however, the NLC droplet structure exhibits a continuous transformation upon application of an electric field.

Another "easy" configuration, a radial one [Fig. 1(b)], formed at the homeotropic anchoring, has been studied in Refs. [9,26–29]. In this configuration, the NLC droplet structure exhibits an abrupt transition, when the electric field E exceeds some critical value E_c, at which the point defect is transformed into a ring one, forming an axial droplet structure [Fig. 1(c)] [30]. However, below this critical value, the director reorients along the field in most of the droplet, with a simultaneous emergence of the wall perpendicular to the direction of the applied voltage and crossing the point defect—a hedgehog in the droplet center. Thus, the structure does not remain unchanged below the critical value of the electric field, which makes it hard to use this configuration in practice.

At the same time, droplets with intermediate conical boundary conditions (CBCs) show the most promising properties. Structures with two boojums and a ring surface defect [7,31,32] or with two boojums and a point defect inside the bulk [7] are observed within such droplets. It has been shown in Ref. [33] that a bipolar axis oriented along the electric field inside the nematic droplets with two boojums and a ring defect [axial-bipolar structure; Fig. 1(d)] can occur. Recently, PDLC films with conical boundary conditions at the interface have been obtained [34].

*vurdizm@gmail.com

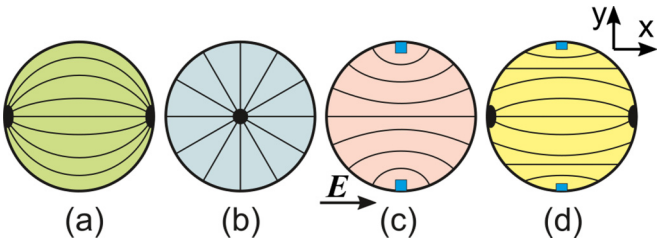

FIG. 1. Director configurations in an equatorial cross section of nematic oblate droplets: (a) bipolar, (b) radial, (c) axial, and (d) axial-bipolar. The XY-coordinate plane coincides with the PDLC film plane here and below.

In the present paper, we study the electrically induced reorientation of the axial-bipolar structure within oblate PDLC droplets (axis ratio $x : y : z = 2 : 2 : 1$) filled with a NLC. Two types of boundary conditions were examined: (i) degenerate planar anchoring as a typical experimental case, and (ii) intermediate conical anchoring, corresponding to the experimental data presented below. We use the extended Frank elastic continuum approach with Monte Carlo annealing optimization [35] to estimate the total free energy. This approach includes the effects of the director field distortion and the formation of defects in the droplet. The interaction between the LC and the surface of a droplet was adopted to utilize conical surface anchoring conditions,

$$F = \int_V \left[\frac{K_{11}}{2}(\mathrm{div}\,\mathbf{n})^2 + \frac{K_{22}}{2}(\mathbf{n}\cdot\mathrm{rot}\,\mathbf{n})^2 + \frac{K_{33}}{2}[\mathbf{n}\times\mathrm{rot}\,\mathbf{n}]^2 + \varepsilon_0\Delta\varepsilon[1-(\mathbf{E}\cdot\mathbf{n})]^2 \right] dV + \frac{W}{2}\int_\Sigma [1-\cos^2(\theta_{\mathbf{nk}}-\theta_0)]d\Sigma + F_{\mathrm{def}},$$

where K_{11}, K_{22}, and K_{33} are the splay, twist, and bend elasticity constants, respectively, W is the surface anchoring energy density, θ_{nk} is the angle between the local director $\mathbf{n}$ and surface normal of the droplet $\mathbf{k}$, θ_0 is the preferred angle between $\mathbf{n}$ and $\mathbf{k}$, and F_{def} is the energy of defects calculated by the summation of the point and linear defect energies (see the details in Ref. [35]). We used $\theta_0 = 90^\circ$ for the PBC case and $\theta_0 = 40^\circ$ for the CBC case, according to Ref. [34]. We produced a numerical modeling of the oblate PDLC droplets filled with nematic 5CB with the ratio between long $dx = dy$ and short dz eigenvectors equal to $dx/2$. The ratio between the elasticity constants was set to $K_{11} : K_{22} : K_{33} = 1 : 0.5 : 1.3$ to simulate the nematic 5CB [36]. The linear energy density of the disclination core was set to $f_{\mathrm{line}}^{\mathrm{core}} = 10K_{11}$ [35], and the anchoring strength $\mu = \frac{WR}{K_{11}} = 10^3$ was used for strong anchoring, where $R = 0.5(dx\,dy\,dz)^{1/3}$ is the effective radius of the droplet. The energy-optimal structures at various values of electric field E were calculated independently for two cases of surface anchoring: PBC, $\theta_0 = 90^\circ$ (Fig. 2) and CBC, $\theta_0 = 40^\circ$ (Fig. 3), corresponding to the experimental data presented in this paper. Hereafter, the dimensionless notations for the electric field $e = ER(\varepsilon_0\Delta\varepsilon K_{11}^{-1})^{1/2}$ will be used, where ε_0 is the dielectric constant, and $\Delta\varepsilon$ is the dielectrical anisotropy of 5CB.

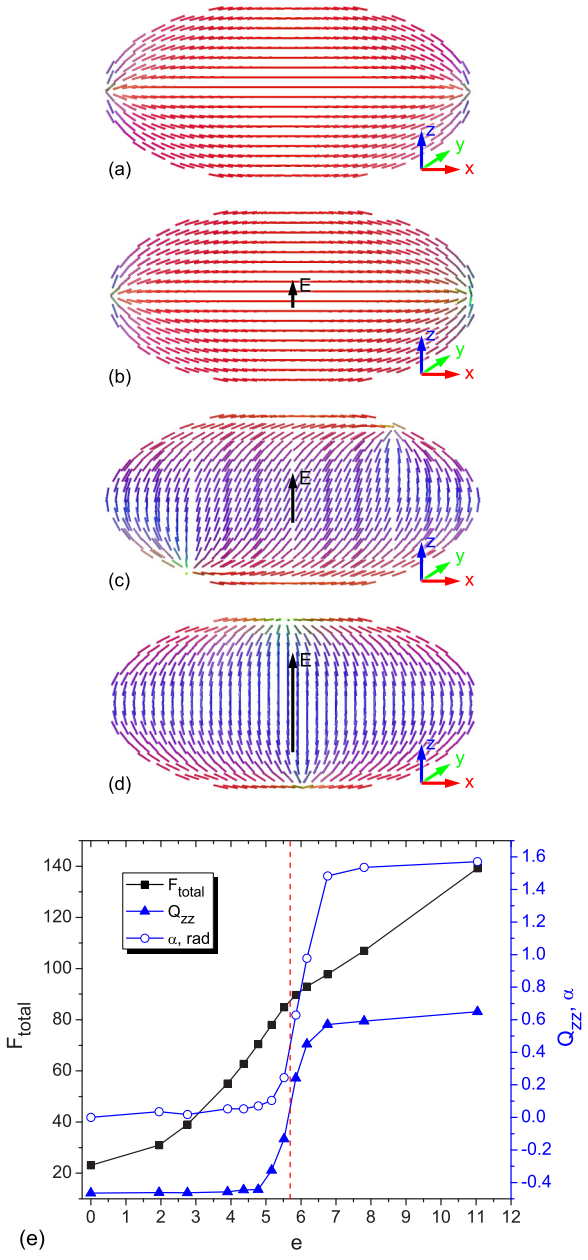

FIG. 2. Droplet structures for $\theta_0 = 90^\circ$ at (a) $e = 0$, (b) $e = 3.9$, (c) $e = 5.9$, and (d) $e = 7.8$. Hereafter, the director vectors are colored in correspondence with the direction (red along the x axis, green along the y axis, and blue along the z axis). (e) Dependencies of the free energy F_{total}, the order parameter Q_{zz}, and the bipolar axis tilt angle α on the dimensionless electric field e. The continuous structural transformation at $e^* \approx 5.7$ is marked with a red dashed line.

The energy-optimal structures in both cases have two boojums belonging to the droplet surface, which are symmetrical with respect to the droplet center, while the tilt angle α of the bipolar axis depends on the value of the electric field. In the absence of electric field the bipolar axis coincides with the long axis of the ellipsoid [Figs. 2(a) and 3(a)]. The structure remains unchanged below some critical value e^* [Figs. 2(b) and 3(b)], with the director field almost undisturbed and the bipolar axis parallel to the long axis of the ellipsoid [see the order parameter

$Q_{zz} = \langle \frac{1}{2}(3n_z^2 - 1) \rangle$ and angle α between the bipolar axis and the long axis of the ellipsoid in Figs. 2(e) and 3(e)]. In the case of PBC ($\theta_0 = 90^\circ$), there is no disclination line, and a continuous structural transformation occurs [see the vertical dashed line in Fig. 2(e)], at which both the director field and the bipolar axis start tilting gradually with increasing electric field [Fig. 2(c)], with the maximum tilt gradient at $e^* \approx 5.7$ and asymptotically reaching $\alpha = \pi/2$ at $e \to \infty$ [Fig. 2(d)].

In the case of intermediate conical anchoring ($\theta_0 = 40^\circ$), the circular disclination line appears, which is nearly perpendicular to the bipolar axis at a small electric field [Fig. 3(b)]. At $e_c \approx 1.75$, the discontinuous structural transformation occurs [see the vertical dashed line in Fig. 3(e)], and both the bipolar axis and circular disclination line abruptly turn by 85°–90° [Fig. 3(c)]. With further increasing electric field, the bipolar axis gradually comes closer to the short axis [Fig. 3(d)], asymptotically reaching $\alpha = \pi/2$ at $e \to \infty$.

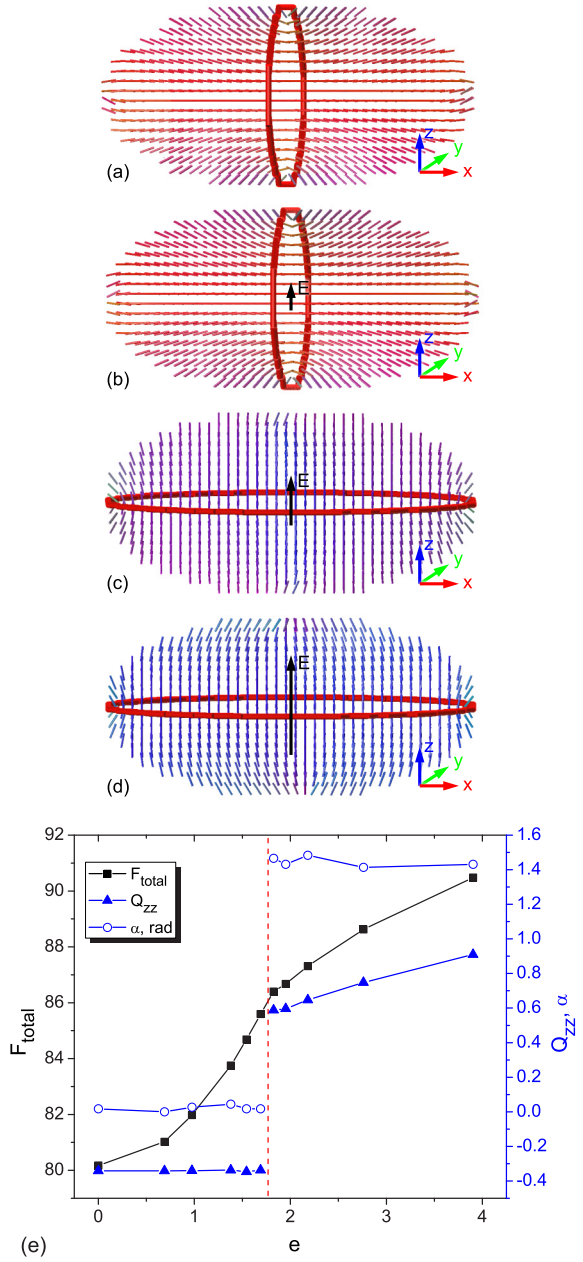

FIG. 3. Droplet structures for $\theta_0 = 40^\circ$ at (a) $e = 0$, (b) $e = 1.7$, (c) $e = 1.8$, and (d) $e = 3.9$. Disclination is shown with a thick red line. (e) Dependencies of the free energy F_{total}, the order parameter Q_{zz}, and the bipolar axis tilt angle α on the dimensionless electric field e. The discontinuous structural transformation at $e_c \approx 1.75$ is marked with a red dashed line.

We have examined experimentally the PDLC film based on the nematic mixture LN-396 (Belarus State Technological University) and poly(isobutyl methacrylate) (PiBMA) (Sigma), assigning the CBC in this mixture where the tilt angle of the director to the surface normal is $\theta = 40^\circ \pm 4^\circ$ [34]. This mixture consists of 5CB (40%), 3OCB (20%), 4OCB (15%), 4CEPO2 (18%), and 4-butyl-cyclohexanecarboxylic acid 3′-methyl-4′-pentyl-biphenyl ester (7%), and presumably has ratios of elastic constants similar to 5CB. The weight ratio of LN-396 to PiBMA was 60 : 40. The electro-optical cell was made by the thermally-induced phase separation (TIPS) method [9], at which the polymer and LC mixture was heated

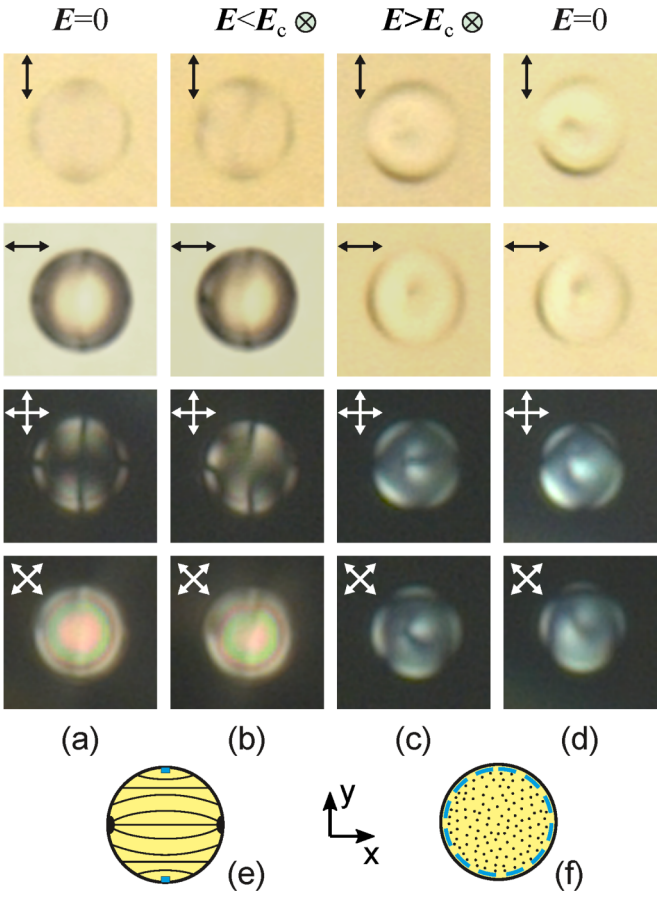

FIG. 4. Polarized optical microscopy images of LC droplet: without the analyzer, made when the polarizer is perpendicular (first row) and parallel (second row) to the bipolar axis; in the crossed polarizers, when the polarizer is parallel (third row) and at a 45° angle (fourth row) to the bipolar axis. (a) Initial state $E = 0$; (b) at $E = 72$ mV/μm; (c) at $E = 80$ mV/μm; (d) in 5 h after switching off. The droplet size in the film plane is 13 μm. The polarizer directions are indicated by the double arrows. The schemes of the director lines and topological defects in the cross section parallel to the film plane are presented for the voltage (e) below and (f) above the threshold value.

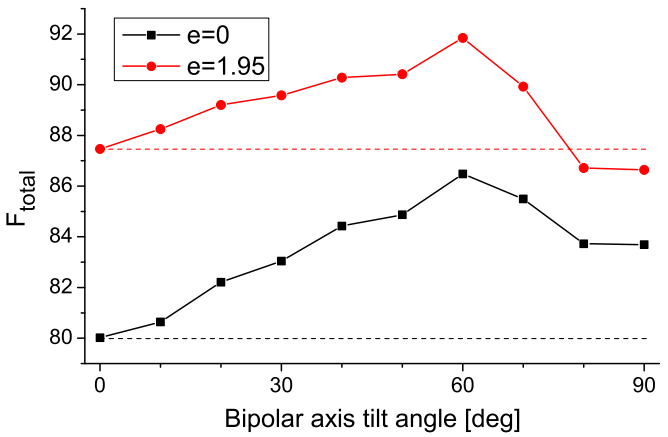

FIG. 5. Dependency of the dimensionless total free energy (F_{total}) of the droplet with $\theta_0 = 40^\circ$ on the bipolar axis tilt angle α at no electric field ($e = 0$) and above the structural transformation ($e = 1.95$). Dashed lines show the value of F_{total} at $\alpha = 0$.

up to 80 °C and then cooled down to room temperature for 1 h. The thickness of the PDLC film was 25 μm, and the LC droplet size was between 10 and 40 μm. The transformation of the orientation structures was studied by the polarizing optical method using an Axio Imager.A1m microscope (Carl Zeiss). An ac voltage of 1 kHz frequency was applied to the cell under study.

An axial-bipolar structure (Fig. 4) is formed within the droplets. Initially, the bipolar axis lies in the film plane [Fig. 4(a)]. There are no visible changes in the orientation structure at electric field strengths up to 64 mV/μm. A slight change of the director orientation in the droplet center starts at 72 mV/μm [Fig. 4(b)], which is approved by the deformation of the extinction bands observed in crossed polarizers. At the same time, the locations of the boojums and of the circular disclination line are practically invariable. A further increase of the electric field up to 80 mV/μm (that is equal in dimensionless form to $e \approx 1.2$) results in an abrupt reorientation of the bipolar axis along the electric field, while the circular disclination line becomes oriented perpendicular to the electric field [Figs. 4(c) and 4(f)]. Surprisingly, the droplet structure fails to restore the initial state, when the electric field is removed. The bipolar axis remains oriented close to the film normal and the whole structure remains the same for several hours after switching off the electric field [Figs. 4(d)]. In contrast to a fully reversible transition in droplets with planar anchoring, it clearly indicates the bistable behavior of the droplets with tilted anchoring.

To understand the cause of the bistability, we calculated free-energy profiles of droplets with CBCs with respect to the bipolar axis tilt angle α (i) in the absence of electric field and (ii) just above the structure transformation, $e = 1.95$. For each value of α, the position of the bipolar axis was fixed, and the rest of the structure was optimized by the same Monte Carlo procedure. The results are shown in Fig. 5. In both cases, there are two minima: at $\alpha = 0$ [the bipolar axis is perpendicular to the electric field, Fig. 3(b)] and $\alpha = \pi/2$ [the bipolar axis is parallel to the electric field, Figs. 3(c) and 3(d)]. These minima are separated by an energy barrier, which accounts for the occurrence of the discontinuous structural transformation and bistability.

To conclude, the degenerate planar and conical boundary conditions were examined for the electrically induced structure transitions in oblate NLC droplets, where the electric field is applied along the short principal axis of an ellipsoidal droplet. To perform computer simulations, the extended Frank elastic continuum approach was expanded for the case of conical boundary conditions. In droplets with PBCs, the interplay between elastic deformations and interactions with the electric field leads to the continuous structure reorientation under the electric field. For the droplets with CBCs, an axial-bipolar structure with a pair of boojums and a circular disclination line is predicted in this case, which hybridizes the axial and bipolar structures of droplets with homeotropic and degenerate planar boundary conditions, correspondingly. In contrast to PBC droplets, in the case of CBC, the addition of a third component, the energy of the disclination line, drastically changes the physics of the electrically induced structural transformation. The unique potential of a bipolar axis tilt with two minima is discovered by the simulations. It results in a discontinuous structural transformation with abrupt changes in the structural and optical properties. The presence of two minima also explains the bistable behavior, discovered experimentally in this system. Another crucial advantage of droplets with CBCs is the decrease of the switching field by multiple times, demonstrated in both computer simulations and experiments. Finally, the studied effect of conical boundary conditions can be important in many systems other than just in PDLC composites. The high sensitivity of the droplets with CBCs to external stimuli (such as light, temperature, shape, etc.) allows its use in the perspective of sensory materials of various types, including liquid solutions, isotropic-nematic solutions, and biological objects.

This study was supported by the joint project of the Russian Science Foundation (Project No. 16-43-03010) and Ministry of Science and Technology of Taiwan (Contract No. MOST 105-2923-E-006-007). The simulations have been performed using the facilities of the Lomonosov Moscow State University Research Computational Center [37].

[1] T. Lopez-Leon and A. Fernandez-Nieves, Colloid Polym. Sci. **289**, 345 (2011).
[2] O. O. Prishchepa, A. V. Shabanov, and V. Y. Zyryanov, Phys. Rev. E **72**, 031712 (2005).
[3] G. H. Springer and D. A. Higgins, J. Am. Chem. Soc. **122**, 6801 (2000).
[4] E. Pairam, J. Vallamkondu, V. Koning, B. C. van Zuiden, P. W. Ellis, M. A. Bates, V. Vitelli, and A. Fernandez-Nieves, Proc. Natl. Acad. Sci. USA **110**, 9295 (2013).
[5] O. Lavrentovich, Liq. Cryst. **24**, 117 (1998).
[6] S. A. Shvetsov, A. V. Emelyanenko, N. I. Boiko, J.-H. Liu, and A. R. Khokhlov, J. Chem. Phys. **146**, 211104 (2017).

[7] G. Volovik and O. Lavrentovich, JETP **58**, 1159 (1983).
[8] J. W. Doane, N. A. Vaz, B. Wu, and S. Žumer, Appl. Phys. Lett. **48**, 269 (1986).
[9] P. Drzaic, *Liquid Crystal Dispersion* (World Scientific, Singapore, 1995).
[10] H.-S. Kitzerow, Liq. Cryst. **16**, 1 (1994).
[11] J. Doane, *Liquid Crystals—Applications and Uses* (World Scientific, Singapore, 1990), Vol. 1.
[12] J. W. Doane, A. Golemme, J. L. West, J. B. Whitehead, Jr., and B.-G. Wu, Mol. Cryst. Liq. Cryst. Incorporating Nonlinear Opt. **165**, 511 (1988).
[13] N. H. Cho, P. Nayek, J. J. Lee, Y. J. Lim, J. H. Lee, S. H. Lee, H. S. Park, H. J. Lee, and H. S. Kim, Mater. Lett. **153**, 136 (2015).
[14] T.-C. Hsu, C.-H. Lu, Y.-T. Huang, W.-P. Shih, and W.-S. Chen, Sens. Actuators, A **169**, 341 (2011).
[15] X. H. Sun and X. M. Tao, Opt. Laser Technol. **43**, 820 (2011).
[16] D. McPhail, M. Straub, and M. Gu, Appl. Phys. Lett. **86**, 051103 (2005).
[17] P.-C. Wu, E.-R. Yeh, V. Y. Zyryanov, and W. Lee, Opt. Express **22**, 20278 (2014).
[18] O. O. Prishchepa, A. V. Shabanov, V. Y. Zyryanov, A. M. Parshin, and V. G. Nazarov, JETP Lett. **84**, 607 (2006).
[19] P. S. Drzaic, J. Appl. Phys. **60**, 2142 (1986).
[20] M. Ambrožič, P. Formoso, A. Golemme, and S. Žumer, Phys. Rev. E **56**, 1825 (1997).
[21] A. V. Koval'chuk, M. V. Kurik, O. D. Lavrentovich, and V. V. Sergan, JETP **67**, 1065 (1988).
[22] A. V. Shabanov, V. V. Presnyakov, V. Y. Zyryanov, and S. Y. Vetrov, JETP Lett. **67**, 733 (1998).
[23] A. Shabanov, V. Presnyakov, V. Zyryanov, and S. Vetrov, Mol. Cryst. Liq. Cryst. **321**, 245 (1998).
[24] O. O. Prishchepa, A. M. Parshin, A. V. Shabanov, and V. Y. Zyryanov, Mol. Cryst. Liq. Cryst. **488**, 309 (2008).
[25] R. H. Reamey, W. Montoya, and A. Wong, Proc. SPIE **1665**, 2 (1992).
[26] R. Ondris-Crawford, E. P. Boyko, B. G. Wagner, J. H. Erdmann, S. Žumer, and J. W. Doane, J. Appl. Phys. **69**, 6380 (1991).
[27] S. Candau, P. L. Roy, and F. Debeauvais, Mol. Cryst. Liq. Cryst. **23**, 283 (1973).
[28] V. Bodnar, O. Lavrentovich, and V. Pergamenshchik, JETP **74**, 60 (1992).
[29] S. Kralj and S. Zumer, Phys. Rev. A **45**, 2461 (1992).
[30] P. Khayyatzadeh, F. Fu, and N. M. Abukhdeir, Phys. Rev. E **92**, 062509 (2015).
[31] Y.-K. Kim, S. V. Shiyanovskii, and O. D. Lavrentovich, J. Phys.: Condens. Matter **25**, 404202 (2013).
[32] J. K. Gupta, J. S. Zimmerman, J. J. de Pablo, F. Caruso, and N. L. Abbott, Langmuir **25**, 9016 (2009).
[33] N. V. Madhusudana and K. R. Sumathy, Mol. Cryst. Liq. Cryst. **92**, 179 (1983).
[34] M. N. Krakhalev, O. O. Prishchepa, V. S. Sutormin, and V. Y. Zyryanov, Liq. Cryst. **44**, 355 (2017).
[35] V. Y. Rudyak, A. V. Emelyanenko, and V. A. Loiko, Phys. Rev. E **88**, 052501 (2013).
[36] G.-P. Chen, H. Takezoe, and A. Fukuda, Liq. Cryst. **5**, 341 (1989).
[37] Supercomputing Center of Lomonosov Moscow State University, http://hpc.msu.ru.